Oligo- and Poly(fullerene)s for Photovoltaic Applications: Modeled Electronic Behaviors and Synthesis

Hugo Santos Silva,[1,2,3] Hasina H. Ramanitra,[2,3] Bruna A. Bregadiolli,[2,4] Didier Bégué,[1] Carlos F. O. Graeff,[2] Christine Dagron-Lartigau,[2] Heiko Peisert,[3] Thomas Chassé,[3] Roger C. Hiorns[5]

[1]Université de Pau et des Pays de l'Adour, IPREM (CNRS-UMR 5254), 2 Avenue Président Angot, Pau 64053, France
[2]Université de Pau et des Pays de l'Adour, IPREM (EPCP, CNRS-UMR 5254), 2 Avenue Président Angot, Pau 64053, France
[3]Institute for Physical and Theoretical Chemistry, Eberhard Karls Universität Tübingen, Auf der Morgenstelle 18, Tübingen 72076, Germany
[4]Departamento de Física – FC – UNESP, Av. Luiz Edmundo Carrijo Coube, 14-01, Bauru 17033-360, Brazil
[5]CNRS, IPREM (EPCP, CNRS-UMR 5254), Hélioparc, 2 Avenue Président Angot, Pau 64053, France
Correspondence to: D. Bégué (E-mail: didier.begue@univ-pau.fr) or R. C. Hiorns (E-mail: roger.hiorns@univ-pau.fr)

Received 13 November 2016; accepted 20 December 2016; published online 3 February 2017
DOI: 10.1002/pola.28502

ABSTRACT: The atom transfer radical addition polymerization (ATRAP) of fullerene to give poly(fullerene)s (PFs) for organic electronics is explored. Quantum chemistry maps the expected electronic behavior of PFs with respect to common electron acceptors, namely fullerene, phenyl-C_{61}-butyric acid methyl ester and its bis-adduct, and mono- and bis-indine-fullerene derivatives. Surprisingly, it is found that PFs should demonstrate electron affinities and LUMO energy levels closer to the bis-derivatives than the mono-adducts, even though only one C_{60} double-bond is used in PF chain formation. A self-consistent library of PFs is synthesized and a correlation between structural characteristics and molecular weights is found. While comonomers with $–OC_{16}H_{33}$ linear side-chains lead to the highest known ATRAP molecular weights of 21000 g mol^{-1}, like-for-like, branched side-chains permit syntheses of higher molecular weights and more soluble polymers. Of the series, however, PFs with $-OC_{12}$ side-chains are expected to be of the greatest interest for opto-electronic applications due to their ease of handling and highest regioregularity. © 2017 Wiley Periodicals, Inc. J. Polym. Sci., Part A: Polym. Chem. **2017**, *55*, 1345–1355

KEYWORDS: atom transfer radical addition polymerization; fullerene; opto-electronic; poly(fullerene)s; structure-property relationship

INTRODUCTION The future of organic photovoltaics (OPV) as a widespread technology will depend on its economic potential, which relates to the efficiencies, manufacturing costs, weight, scalability, and to a large extent, lifetimes.[1] In bulk-heterojunction (BHJ) devices, the junction between the electron donor (p) and electron acceptor (n-type) materials is formed by their blending. The acceptor should display as great a contact surface with the donor molecule, while maintaining a clear percolation path to guide charges to the electrodes.[2,3] Thermal annealing can improve OPV device performances due to the crystallization of both p and n-type domains resulting in enhanced charge mobilities, in addition to an optimization of the phase segregation with respect to charge separation and collection.[4–8] However, as the materials further crystallize, the phases can be coarsened leading to reduced $p-n$ interfaces, hindering device efficiencies. The mixture is inherently unstable and can be easily moved toward the excessive aggregation of fullerenes, based on the simple "like-likes-like" behavior. Controlling this feature of thermal stability is thus a key-parameter in determining OPV efficiencies and lifetimes. Several approaches have been taken to manage this aggregation, and include processing techniques such as thermal and solvent annealing, and the employment of molecular additives,[9–14] and macromolecular compatibilisers.[15–19]

An another route to stabilizing the active layer is by polymerizing C_{60} to give poly(fullerene) (PF) acceptors that are soluble in the matrix, without losing distinctive domain formation. Main-chain PFs are prepared either by the polyaddition of a symmetrically difunctionalized monomer and fullerene, for example such as in the sterically controlled azomethine ylide polymerization,[20] or the reaction of a premodified fullerene bisadduct and a difunctionalized comonomer.[21] The former

Additional Supporting Information may be found in the online version of this article.

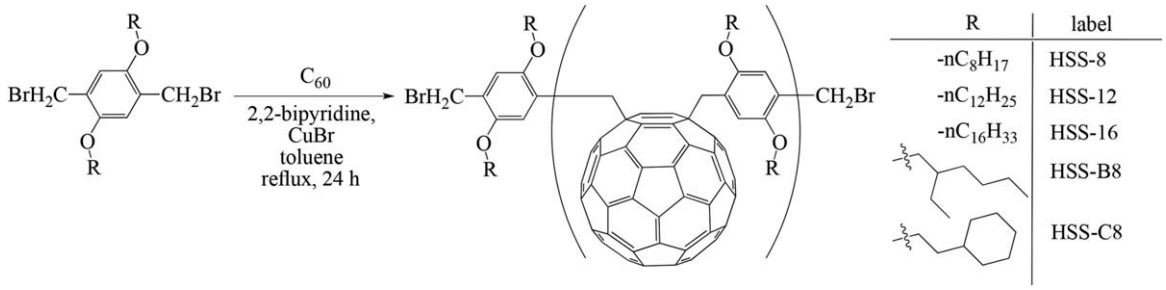

SCHEME 1 The general ATRAP reaction scheme with the labels used for the library of PFs prepared in this study.

method is more readily transferred to industry as the PFs are prepared in a one-pot reaction. However, a challenge arises with this route as there are eight possible stereoisomers resulting from bis-additions around the C_{60} sphere,[22] and these variations can negatively impact on the electronic properties.[23] Furthermore, the formation of multi-adducts should be avoided as they lead to crosslinked polymers that display greatly reduced solubilities and higher retention of impurities.

Prior work has shown that polymers can be grafted onto C_{60} using atom transfer radical additions with Br-terminated polymer chains.[24–27] It is possible to control the points of addition of the polymers to just one phenyl ring on the fullerene sphere due to a mechanism of bromine transfer between radical states.[28] The discovery that it was possible to replace a polymer by a small bis-functional molecule means that main-chain oligo(fullerene)s and PFs can be prepared using this chemistry.[29] Theoretically, it is possible to produce only one type of isomer along the polymer chain, favoring the synthesis of materials with well-defined electronic properties. This so-called atom transfer radical addition polymerization (ATRAP) is facile, lends itself to the preparation of block copolymers,[30] and can be extended to various C_{60} derivatives such as phenyl-C_{61}-butyric acid methyl ester (PCBM).[31] However, only one polymer has been prepared using ATRAP, and the properties remain poorly understood. Here, we present the expected electronic properties of ATRAP-based PFs with respect to those of established bis-adduct materials. These results justify the synthesis of these materials, since the acceptor electronic properties remain almost unchanged compared to benchmark C_{60}-based acceptors. We also explore, from a synthetic point of view, the effect of using various types of comonomers on the ATRAP reaction, as shown in Scheme 1. The proposed ATRAP mechanism is fully detailed in the supporting information (Supporting Information, Figure S1). In effect, the polymerization is a polycondensation, however, it may also follow an equilibrium which can shift in the direction of the reagents, due to rupture of relatively weak methylene-C_{60} bonds.[27,32]

RESULTS AND DISCUSSION

Prediction of Electronic Properties with Respect to Established C_{60}-Derivatives

To decide whether or not PFs are suitable for OPV use, we determined their electronic properties compared to benchmark materials, namely: PCBM,[33,34] bis-PCBM,[35–38] mono-indene-C_{60} (ICMA), and the indine bisadduct ICBA.[38–40], with the structures detailed in Figure 1. PCBM is a successful acceptor due to its appropriate LUMO level (ca., −4.3 eV),[41] good solubility,[36] high electron affinity (EA), and ability to form semi-crystalline domains that act as as percolation channels.[34] Variations in the lateral chain have been shown to affect solubilities and photovoltaic performances.[40,42] The bis-PCBM derivative increases the photocurrent, raises the LUMO and thus the V_{oc}, and displays improved solubilities.[43] Similarly, the C_{60}-indine derivatives have a higher LUMO, delivering a 40% increase in efficiency against similar PCBM-based devices.[38–40]

So as to make useful comparisons, bis-$PC_{60}BM$, $IC_{60}MA$, and $IC_{60}BA$ were all constructed using the *trans*−1 position (symmetrically opposed to the first attack on the C_{60} sphere) thus reducing the number of modeled molecules and the associated scattering of property values. Their geometries, alongside a representative ATRAP molecule notionally formed using 1,4-dibromomethyl-2,5-diethoxyphenylene comonomer, were fully optimized within the B3LYP/6-31G** level of theory using the Orca 3.0.3 package.[44] LUMO energy levels, vertical and adiabatic electron affinities, electrophilicities, reorganization energies, and transfer integrals were calculated. These values (except for transfer integrals) are relative to those of C_{60} and are reported and discussed in the following sections. It should be noted that diffuse functions were not used because of electron density convergence problems for fullerene-based materials in the anionic state. Treitel et al. indicated that molecules with extended conjugation do not need these functions for calculating electron affinities.[45]

LUMO Energy Analyses, Electron Affinities, and Electrophilicities

The yield of an OPV device is proportional to the short-circuit current (J_{sc}) and the open-circuit voltage (V_{oc}).[46] Thus, increasing the V_{oc} provides a route to improving OPV efficiencies. The V_{oc} is proportional to the difference between the energy of the HOMO of the p-type material and the n-type LUMO. To overcome Coulombic interactions between the excited electron and hole, a threshold value of about 0.2-0.5 eV in the gap between the p-type LUMO and n-type LUMO is required.[47] The V_{oc} can thus be tailored by preserving this gap and raising the LUMO of the n-type material. This, in itself, reveals that a universal n-type material is not a realistic concept. Controlling the depth of the LUMO energy level needs to take into account prarameters arising from: molecular symmetry, the presence of electron-poor groups, electronic

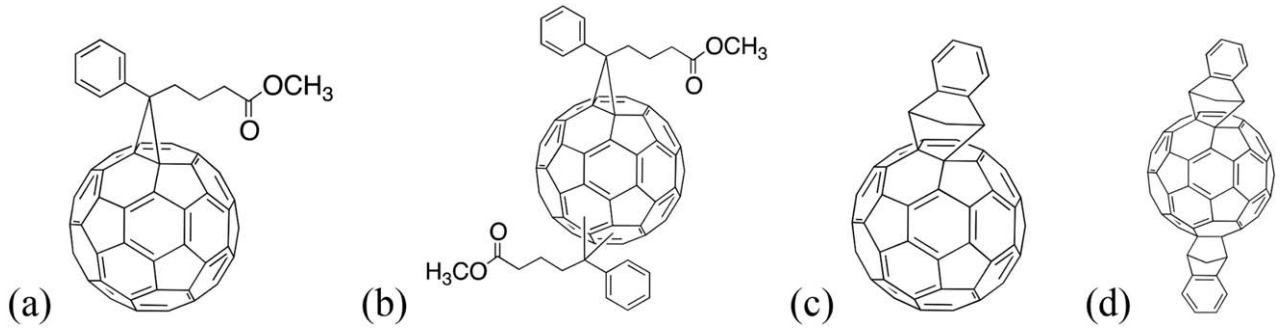

FIGURE 1 Structures of fullerene acceptors used in this comparative study: (a) PCBM, (b) bis-PCBM, ICMA, and ICBA.

resonances and open-shell configurations, amongst others.[48–50] Any disruption of the electronic structure and/or molecular geometry of C_{60} will lead to molecules with a shallower LUMO level.

It should be noted that LUMO orbital energies calculated by density functional theory (DFT) should not be taken as absolute because of the non-wave-function character of this method and the variational principle.[51,52] Also, identifying the V_{oc} *via* the LUMO energies relies on a one-electron picture, that is, orbital relaxation is not taken into account, and on the validity of the Koopman's theorem. Conversely, the empirical estimation of the LUMO energies is performed by cyclic voltammetry (CV) and these values should not be compared to this orbital energy but to the EA of the molecule. During electronic reduction under CV conditions, there is enough time for orbital relaxation to take place and this is more appropriately associated to an EA definition rather than that of the LUMO. Under such situations, we believe that the approach taken by Nardes et al.[53] is a good compromise between a theoretical DFT LUMO estimation and empirical CV indications of LUMOs. These values are important as Brabec et al.[47] showed that the V_{oc} of OPVs are independent of device geometries and film thickness, and strongly correlate to the reduction potential of the fullerene derivative. Lenes et al.[54] showed that the V_{oc} of a polymer-fullerene cell has a negative linear relation with the first reduction potential of the n-type molecule used only for devices with ohmic contacts.

Using Janak's definition of EA, one has ($EA = E(N_0)\text{-}E(N_{+1})$) where N_0 is the number of electrons in the ground state and N_{+1} is the state with an extra electron. Not only the EA, but the resistance against electron back transfer to a donor molecule is an important parameter to consider. Anafcheh et al.[55] showed that, generally, there is a linear correlation between experimental V_{oc}s and theoretically-calculated LUMOs and EAs. One can also define a global index for the electrophilicity strength of a system as defined by Parr et al.[56] This index correlates the quantitative chemical concepts of the electronic chemical potential (μ) and hardness (η). Each quantity can then be assigned as a basis for evaluating how electrophilic a system is by using μ to measure the propensity of the system to acquire an additional electron from adjacent electron-rich species, and by means of η to describe the resistance of the system to exchange this electron with the environment.

The chemical quantities μ and η are defined, within a constant external potential $v(r)$ (vertical regime) as:[56]

$$\mu=\left(\frac{\partial E}{\partial N}\right)_{v(\vec{r})},\ \eta=\left(\frac{\partial^2 E}{\partial N^2}\right)_{v(\vec{r})}$$

Assuming the differentiability of $E(N)$, the expansion around N_0 using the definitions of μ and η gives:

$$E(N)=E(N_0)+(N-N_0)\mu+(N-N_0)^2\frac{\eta}{2!}+(N-N_0)^3\frac{\gamma}{3!}+\ldots$$

Using a finite difference approximation and considering a quadratic $E = E(N)$ curve, μ and η can be given by:

$$\mu=\frac{E(N+1)-E(N-1)}{2}$$

$$\eta=E(N-1)+E(N+1)-2E(N_0)$$

or:

$$\mu=\frac{-(\mathrm{IP}+\mathrm{EA})}{2}$$

$$\eta=\mathrm{IP}-\mathrm{EA}$$

Effectively, μ is defined as the opposite to Mulliken's definition of electronegativity. Finally, the electrophilicity (ω) can be defined by $\omega \equiv \mu 2/2\eta$. This is proposed in analogy to the power equation of classical electricity (power $\equiv W = V^2/R$ where V is the voltage at the terminal of any given resistor of resistance R). With this, one can think of ω as an "electrophilic power," as originally described by Parr et al.[56] Table 1 shows the calculated values of these properties.

Comparing the benchmark molecules to C_{60}, no matter which chemical modification is made to the sphere, there is always a decrease in electron acceptor properties (*in vacuo*). This does not take into account the presence of a donor polymer. Also, based on the decrease in η, the modified molecules should give away electrons more easily than C_{60}. Interestingly, as indicated by Table 1, ATRAP materials although disrupted at only a single double bond, have similar properties

TABLE 1 Electronic properties of C_{60} derivatives

	LUMO (eV)	$EA_{vert.}$ (eV)	$EA_{adiab.}$ (eV)	μ (eV)	η (eV)	ω (eV)
C_{60}	0.00	0.00	0.00	−4.45	5.22	1.90
PCBM	0.13	−0.07	−0.06	−4.21	4.88	1.82
bis-PCBM	0.24	−0.11	−0.11	−4.06	4.67	1.77
ICMA	0.15	−0.09	−0.10	−4.19	4.88	1.80
ICBA	0.28	−0.17	−0.18	−4.01	4.68	1.72
ATRAP	0.23	−0.11	−0.07	−3.94	4.41	1.76

LUMO energy levels and electron affinities (EA) are indicated relative to those of C_{60}. The ATRAP model carries ethoxy side-chains. See text for definitions of terms.

to the benchmark bis-adducts that have two disrupted bonds. This may be due to the presence of the comonomer on the ATRAP model, which through its localized HOMO has a pronounced and selective influence on the chemical potential, hardness, and electrophilicity rather than on the LUMO or EA values.

Reorganization Energies, Intra-Chain Transfer Integrals, and Mobilities

The aforementioned properties do not take into account the contribution of the environmental molecules and any geometrical reorganization induced by charge acceptance. To account for these effects, the semi-classical Marcus theory proposes a well-documented model to estimate their impact on charge transfer.[57] The mobility (ξ) is defined in function of the charge-transfer rate k_{CT} as:

$$\xi = \frac{ea^2}{2k_B T} k_{CT}$$

$$k_{CT} = \frac{2\pi}{\hbar^2} t^2 \sqrt{\frac{1}{4\lambda\pi k_B T}} \exp\left[\frac{-(\Delta G^0 + \lambda)^2}{4\lambda k_B T}\right]$$

where k_B, T, a, e, t, $\hbar$, λ are the Boltzmann constant, temperature, transport distance, electronic charge, the transfer integral, the reduced Planck's constant, and the inner reorganization energy, respectively. The value of a is obtained from a quantum-chemistry geometry optimization. ΔG^0 stands for the difference in the Gibbs free energy of the system before and after the charge-hopping process and is equal to zero if the molecular segments are equal. The reorganization energy λ comes from the vibrational structural change due to the electron gain/loss process with the segment and is composed of two terms: $\lambda = \lambda_1 + \lambda_2$, which are, respectively, the energy difference due to the structural relaxation of gaining one electron by the molecular structure and the energy difference of losing one electron.[58,59] In other words, λ_1 is the difference between the neutral state energy of the ionic state geometry, and the ground state energy of the native state. λ_2 is the difference of the ionic state energy in the ground state geometry and the ionic state energy in the ionic state geometry. Based on this model, and to maximize the mobility of a given material, one must decrease the reorganization energy for a given temperature and interatomic distance. This is straightforward in terms of the concept of energy payback. As we are interested in an electron-gain process, only the significant anionic species have their reorganization energies presented in Table 2. One can note that the effect of the modification of fullerene is the same as presented above: there is an increase in the reorganization energies for both the benchmark and ATRAP molecules. Generally speaking, ATRAP molecules should have reorganization energies that are around twice those of C_{60}.

The transfer integral t of a given system is related to the energetic splitting of electronic levels, attributed to the interaction between adjacent segments. For an electron-hopping process, this is given by $t = (1/2)\sqrt{(E_{L+1} - E_L)^2 - (\varepsilon_1 - \varepsilon_2)^2}$. E_{L+1} and E_L are the energies of the LUMO + 1 and LUMO molecular orbitals of the interacting segments (representing the splitting of the individuals LUMOs due to the interaction) and ε is the total energy of the molecular segments. As they are equal, $\varepsilon_1 = \varepsilon_2$. A final form of the equation is $t = (1/2)|E_{L+1} - E_L|$.

To estimate intra-chain transfer integrals using DFT methodologies,[60] dimers in Figure 2 were constructed. They can adopt both *cis* and *trans* conformations and each one was fully optimized within the HF-3C level of theory, followed by B3LYP/6-31G** single-points to estimate the LUMO(+1) splittings. With this in hand, we estimated electron mobilities for dimers using the reorganization energy values obtained from analogous monomers, that is, the bis-adduct fullerenes. While this is not the most preferred methodology as there are two different methods being used to simultaneously solve the Marcus equation and because the reorganization energy is not calculated for the dimers, it does, however, clearly indicate that the electron mobility is generally lower in *trans* configurations (Table 3). In a real system, both configurations are assumed to coexist, inducing a spread in electron mobility along one chain.

The ensemble of these electronic structure calculations allowed us to foresee that PFs are indeed suitable for use in OPVs based on the fact that their acceptor electronic properties are comparable to those found for other C_{60} benchmark materials. The reorganization energy is the most affected parameter but this is due to the presence of the comonomer

TABLE 2 Electronic properties of C_{60} derivatives

	λ_1^{anion} (meV)	λ_2^{anion} (meV)	λ_T^{anion} (meV)
C_{60}	69.7	65.6	135.4
PCBM	70.3	73.6	143.9
bis-PCBM	79.5	75.8	155.3
ICMA	70.5	65.0	135.5
ICBA	70.3	65.9	136.1
ATRAP	112.0	108.1	220.1

ATRAP model carries ethoxy side-chains.

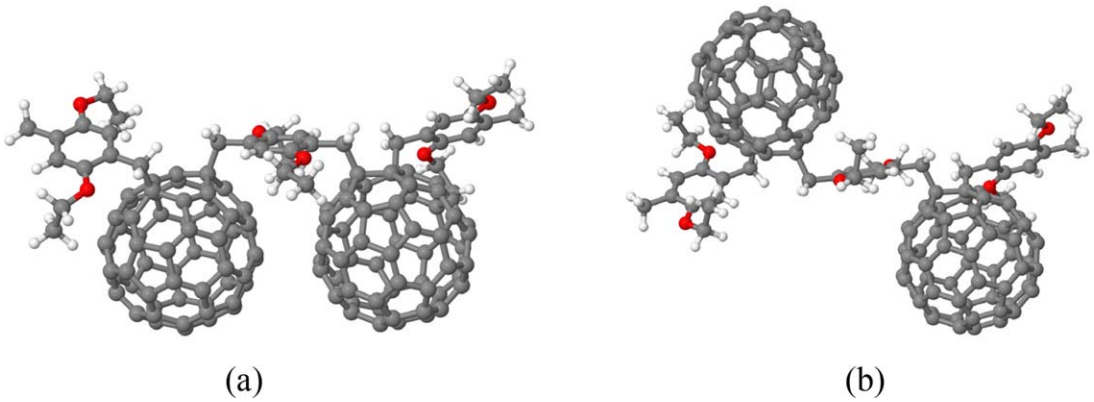

FIGURE 2 ATRAP dimers in: (a) *cis* and (b) *trans* conformations with comonomers where R = -OCH_2CH_3. PCBM, (c) ICMA, and (d) ICBA. [Color figure can be viewed at wileyonlinelibrary.com]

that also might play a role on the charge accomodation on the fullerene sphere but is still of the same order of magnitude as PCBM. Indeed, the LUMO, $EA_{vert.}$, $EA_{adiab.}$, and ω of PFs are very much comparable to those found mainly for bis-PC_6M and $IC_{60}BA$. These encouraging results motivated their synthesis with a large range of lateral chains so that

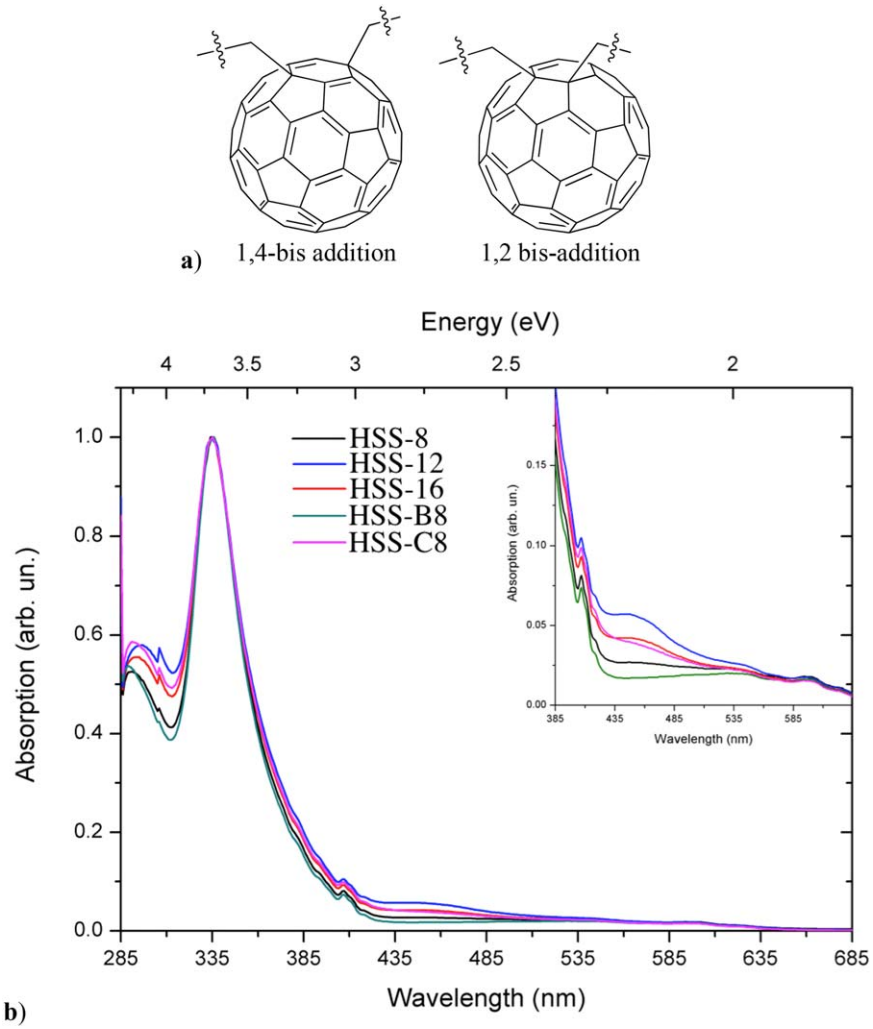

FIGURE 3 a) Positions of 1,4- and 1,2-bis additions; and b) UV-visible optical absorptions for the synthesized macromolecules (THF, ambient temperature). [Color figure can be viewed at wileyonlinelibrary.com]

TABLE 3 Fullerene inter-distance, transfer integral, and intra-chain mobilities for both ATRAP isomers carrying ethoxy side-chains

	a (Å)	Transfer Integral (meV)	Mobility ($cm^2\ V^{-1}\ s^{-1}$)
cis	10.16	36.7	1.88×10^{-6}
trans	13.78	9.1	2.12×10^{-7}

their electronic and morphological properties could also be screened. Their syntheses are thus described in the next section.

Syntheses

Prior work demonstrated the efficiency of polymerizing comonomers of the type 1,4-dibromomethyl-2,5-dialkoxyphenylene with C_{60} to form oligomeric and polymeric structures in appreciable quantities, however, only one comonomer type—carrying methyloxy(cyclohexyl moieties)—was used.[29,30] To map out variations in properties with different alkyl chain lengths, we sought to prepare the self-consistent library shown in Scheme 1. *n*-Octyloxy, *n*-dodecyloxy, and *n*-hexadecyloxy lateral groups were chosen to explore the effects of chain-lengths, while 2-ethylhexyloxy and ethyloxy(cyclohexane) where used to study the effect of steric bulk with respect to the same number of carbon atoms as the *n*-octyloxy moieties. The lateral chains were chosen with the knowledge that very small comonomers such as α,α-dibromoxylene result in numerous additions to the C_{60} and extensive crosslinking, while bulky groups can facilitate limited additions through steric repulsion over the C_{60} surface. It was expected that the longest alkyl chains would also influence solid-state phase separations leading to high electon mobilities,[61,62] and may even induce liquid-crystal behavior, which might also present lamellar structures.[63–67]

The chosen library of comonomers were all easily accessible following chemistry deatiled elsewhere[20] and shown in Scheme 2.

The purification was simplified by Soxhlet washing so that the product had limited contact with air. Acetone removed 2,2′-bipyridine, CuBr and $CuBr_2$. A second wash with *n*-hexane removed unreacted C_{60}. Similarly, Soxhlet extraction appeared to be the easiest way to recover the synthesized product.[68] We tried other techniques such as: precipitation of the reaction product in methanol and *n*-hexane followed by filtration; and silica column extraction with *n*-hexane, toluene and chlorobenzene phases.[32,69] The former technique yielded C_{60}-rich samples contaminated with residual copper(II) bromide, while the latter efficiently separated unreacted C_{60}, polymerized material, insoluble highly cross-linked phases, copper salts, but also exposed the crude material to light and air. It is worth noting that C_{60}-based materials can undergo crosslinking either by oxidation[70] or reaction with UV light.[71] Given this, Soxhlet extraction was the most appropriate purification technique as it can be performed in the dark and under inert atmosphere. Full details of the synthetic procedures and yields are in the Supporting Information.

Characterizations

UV-visible spectroscopy was used to characterize the C_{60} products. Back in 1997, Okamura et al.[72] based on yet earlier work[73,74] found that the UV-visible properties of modified fullerenes are dependent on the relative positions of substitution. They were able to show that 1,4-bis adducts exhibit a broad absorption at around 440 nm, while 1,2-bis adducts generally have a sharp absorption around 430 nm. The positions of addition to C_{60} are shown in Figure 3(a). It should be noted that C_{60}, while generally thought insoluble in THF, can also, at very low concentrations, give a peak at around 400 nm.[75] In general, it was expected that 1,4-bis adducts would result from the ATRAP due to steric effects. Zooming in the specific region of around 445 nm of Figure 3(b), one can find the same characteristic broad peak described by Okamura et al.[72] and Kadish,[76–79] and considered a diagnostic indicator of the synthesis of 1,4-bis-attacked fullerene moieties. There is also a peak at around 400 nm, which might be indicative of the presence of C_{60} or 1,2-adducts, the peak having shifted with the solvent. As both are possible, the size of the broad peak at 445 alone is the best indicator of the proportion of 1,4-addition products in the polymer chain. The HSS-12 comonomer gives the strongest evidence of this attack followed by HSS-16 and HSS-B8, with HSS-C8 and HSS-B8 oligomers far behind, suggesting that the comonomer with the $-OC_{12}$ side-chains gives the most regular additions.

Figure 4 shows the THF elution curves of the samples. Products labeled (f_2) are from *n*-hexane soluble phases recovered from after the initial Soxhlet washes and carry unreacted C_{60}. SEC experiments were performed using chlorobenzene or THF eluents. The solubilities of the PFs were variable in THF but remained more comparable in chlorobenzene, giving the values of M_n and M_w in Table 4. It should be noted, however, that while self-consistent, these SEC indicated values are, however, erroneous. It is known that there is a very different hydrodynamic volume between polystyrene standards and C_{60} derivatives so that, for example, C_{60} commonly elutes after toluene when using THF as eluent.[80] A more realistic estimation of the peak molecular weights (M_p) of the samples can be obtained by visual inspection of the curves. This methodology was developed by Gügel et al.[81] Each subsequent shoulder or peak is assumed to indicate a macromolecule with an additional more repeating unit. The values of M_p are thus calculated using this methodology and

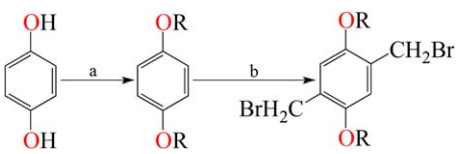

SCHEME 2 General synthetic route used to obtain 1,4-dibromomethyl-2,5-dialkoxyphenylene comonomers. Notes: (a) RBr, K_2CO_3, acetone, reflux; and (b) HBr, paraformaldehyde, acetic acid, heat. [Color figure can be viewed at wileyonlinelibrary.com]

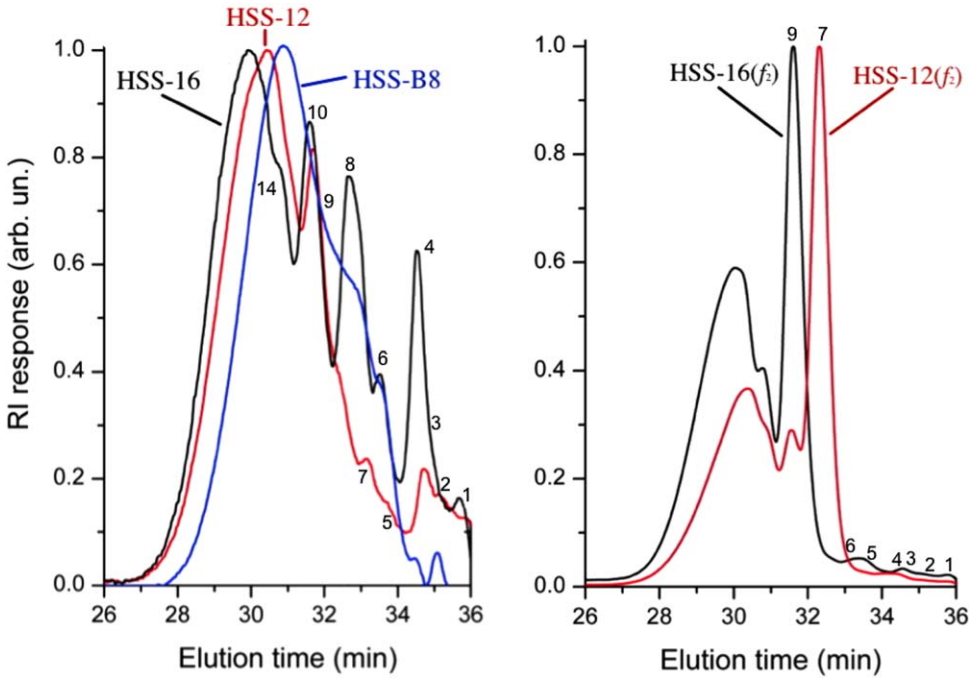

FIGURE 4 SEC (THF, RI, 30 °C) with labels marking each peak and shoulder: left, the most soluble of the PFs, namely HSS-B8, HSS-12, and HSS-16; and right, the *n*-hexane fractions (f_2) extracted from HSS-12 and HSS-16 purifications. SEC-THF traces for the most THF soluble materials (a) and for the *n*-hexane soluble phases extracted (b) from HSS14 and HSS14 purifications. [Color figure can be viewed at wileyonlinelibrary.com]

are also given in Table 4. Clearly the longer the alkyl side-chain, the higher the molecular weight of the product. This results from two factors: first, steric hindrance caused by the lateral chain enables fullerenes to more easily form linear chains and avoid crosslinking; and second, the molecular volume of the lateral group is vital to the solubility of the as-formed molecules, helping them remain in solution to contribute to further addition reactions. Those with short side-chains, however, precipitate out from the reaction medium at low molecular weights. That of HSS-16 is to our knowledge by far the highest yet prepared using the ATRAP route. By comparing values, and in accordance with work on other PFs,[24] the SEC values of M_n and M_w calculated against polystyrene standards should be multiplied by a factor of between 3 and 8 to attain a value closer to reality. The dispersities ($Đ = M_w/M_n$) of the samples are lower than 2 (the expected value for polycondensations) due to the purification process. It is also interesting to note the impact of the side chains on the contents of the *n*-hexane soluble phases recovered during purification (denoted f_2). For the products HSS-8, HSS-B8, and HSS-C8, this *n*-hexane extraction was found by ^{13}C NMR (*vide infra*) to consist of unreacted C_{60}, while *n*-hexane extractions from HSS-12 and HSS-16 consisted mainly of fullerene bis-adducts.

TABLE 4 SEC indicated molar masses where M_p has been calculated using self-consistent PF peak calibration (THF, 30 °C), and, for comparison, M_n and M_w against polystyrene standards (chlorobenzene, 50 °C)

Sample	M_p (g mol^{-1}) (repeating units)	M_n (g/mol)	M_w (g/mol)	$Đ$
HSS-8	—	920	1290	1.40
HSS-12	16700 (14)	2990	4900	1.64
HSS-16	21000 (16)	3110	4610	1.48
HSS-B8	13000 (12)	970	1750	1.81
HSSC8	—	560	810	1.45
HSS-12(f_2)	8330 (7)	1860	3110	1.68
HSS-16(f_2)	11750 (9)	2500	3740	1.50

Note: HSS-8 and HSS-C8 were not soluble enough to give clearly discernable peaks.

On comparing the oligomers and polymers arising from the lienar (HSS-8), branched (HSS-B8) and cyclic (HSS-C8) comonomers, we find that the order of increasing molecular weight is HSS-C8 < HSS-8 < HSS-B8, with the latter providing by far the largest and most soluble polymers. However, they are not as long as those arising from longer linear chains such HSS-12, indicating that the positive effects of branched side-chains can be limited.

In general, NMR characterizations were hampered by the low solubility of the polymeric materials, the long relaxation times of quaternary carbons, and the tendency of the molecules to aggregate such that increasing concentrations did not necessarily improve signal qualities. Samples were prepared using low power sonication and filtering through 45 μm PTFE membranes. Long acquisition times and extended

cycles were required for both proton and especially carbon signals (D1 = 10 s, > 4000 cycles).

Considering the ^{1}H NMR (Supporting Information Figures S3 and S4) we can see intense peaks due to α-protons in the alkoxy groups at about 3.5–4.0 ppm. Two peaks at 7.0 and 7.3 ppm arise from the aromatic comonomer protons. In the first ATRAP works,[29,30] based on what might be considered model systems,[78,79,82] the C_{60}-methylene protons were indicated by a wide double-doublet, around 4.2 ppm ($J = 120$ Hz). Here, we find similar peaks but they are much broader and less resolved than those previously reported. The broadening is associated with varying envirments along the chain for each nucleus; this indicates that the macromolecules are longer than those previously formed. In particular, we find that HSS-12 and HSS-16 are by far the broadest, correlating with the SEC results and confirming their relatively high molecular weights.

As aforementioned, it was nearly impossible to obtain ^{13}C NMR spectra of the products; often only small amounts of C_{60} could be descerned. Therefore, we turned to the hexane fractions (f_2) of HSS-12 and HSS-16. These, containing low molecular weight material, gave spectra (Supporting Information Figure S5) confirming the general repeating unit structure, with peaks arising for the modified C_{60} at about 160–140 ppm, the aromatic comonomer (ca., 128 and 114 ppm), and the comonomer side-chains at lower ppm values. Interestingly, the ^{13}C NMR C_{60} peaks are broader than those of prior work,[30] again confirming the increased molecular weights of these PFs. In the case of HSS-12(f_2), thirty peaks could be observed in the region 160–140 ppm, aside from one arising from a small impurifity of C_{60}. One peak is expected to be associated with the comonomer's quaternary -*C*-O, another with C_{60}, leaving twenty eight due to the in-chain C_{60} moiety. This is in agreement with expectations, given that a comparable bis-adduct, 1,4-$(C_6H_5CH_2)_2$-C_{60} shows the same number of peaks,[82] and confirms the relatively high regioregularity of the PFs. It should be noted that in the case of HSS-16(f_2) additional peaks could be observed at about 141 and 140.5 ppm. These are diussed *vide infra*. The exact degree of regioregularity could not be determined as other peaks may be hidden by those seen, and in any case, integration of ^{13}C NMR cannot be performed with certainty.

Two-dimensional HMBC NMR were also performed on HSS-12(f_2) and HSS-16(f_2) samples, as shown in Supporting Information Figure S6 in the Supporting Information. Correlations due to the –CH_2Br group (4.46;29), and the diasosterotopic C_{60}–CH_2– protons at (4.35;43) and (3.98;43) are clearly visible, confirming the polymer structure. Of interest are the C-O-C*H*$_2$- protons correlating at (4.1;68) and (3.7;69) indicating that the side-chains are also held within a constrained environment by the proximate C_{60}s.

CV was used to study the electronic affinity of the PFs, and the results are summarized in Table 5. As expected, all are very similar, within at least 0.03 eV of one another. This is not unusual given the relatively small changes in their character and position; future work will consider a broader range of comonomers. Additionally, these values corroborate the aforementioned modeling in that all LUMO energy levels are higher than that of PCBM by around 0.4 eV, confirming the interest of these materials for OPV applications. This would tend to suggest that 1,4-modification of a C_{60} phenylene group is possibly a powerful method to alter C_{60} EA. However, one sample does stand out from the others and that is HSS-16f2, which is higher than PCBM by around 0.6 eV. This fraction was collected at the start of the purification process using a poor solvent, that is, hexane, to remove impurities. So while interpretation of this data is difficult as it may contain a mixture of materials, it may hint that a small proportion of low molecular weight tetra-adducts are formed with the –OC_{16} comonomer and that these are responsible for this very high LUMO. This possibility of the presence of tetra-adducts is further hinted at by the aforementioned presence of extra peaks in the ^{13}C NMR of HSS-16(f_2), however this should be treated with caution given that this is an impure fraction.

TABLE 5 Cyclic voltammetry of PFs and PCBM prepared using 1,2-dichlorobenzene/acetonitrile (4:1 v/v) solutions in the presence of tetrabutylammonium hexafluorophosphate (0.1 M)

Molecule	E_1 (V)	E_2 (V)	$E_{1/2}$ (V)	E_{LUMO} (eV)
HSS-8	−1.35	−1.49	−1.42	−3.38
HSS-B8	−1.35	−1.48	−1.41	−3.39
HSS-C8	−1.35	−1.48	−1.41	−3.39
HSS-12f1	−1.35	−1.49	−1.42	−3.38
HSS-16f1	−1.34	−1.45	−1.39	−3.41
HSS-16f2	−1.58	−1.71	−1.64	−3.16
PCBM[a]	−0.97	−1.04	−1.0	−3.8

Note: a) PCBM values taken from ref. 20(b) in which the experiment was performed under the same conditions as those used here.

Thermal gravimetric analysis was used to follow the thermal degradation profile of the PFs. While the thermograms shown in Supporting Information Figure S8 may initially seem dissimilar, the first differentials of the thermal process show a comparable set of four peaks occuring in each sample. The first peak, around 80 °C, is associated with residual solvent evaporation.[32] The second, at 290 °C is associated with the loss of comonomer side-chains, representing approximately 50% of the whole weight. The third peak, around 380 °C is consistent with the C_{60} release reported by Pozdnyakov et al.[32] The last peak at 440 °C is possibly due to the departure of —CH_2Br groups. These degradation profiles are consistent with those found previously for polystyrene stars with C_{60} cores.[25,27,28,32] Without chromatographic techniques, a complete corroboration of the degradation products is not possible. However, an attempt was made to better identify the origin of each degradation step by running comparable characterizations of the precusors of

HSS-12, i.e., 1,4-bis(dodecyloxy)benzene (**3**) and 1,4-bis(bromomethyl)−2,5-bis(dodecyloxy)benzene (**4**) (Supporting Information Figure S9). In the case of the former, the loss of alkoxy side-chains is suggested with an onset of around 260 °C; for the latter, this process is accelerated by the presence of $-CH_2Br$ groups, which themselves can be inferred from %wt changes to be lost as $\dot{C}H_2Br$ groups perhaps between 320 and 480 °C.[83] These results would tend to confirm the above observations. Differential scanning calorimetry was attempted with all samples, however, none showed any clear characteristics within the range treated. A representative sample, that of HSS-12, is shown in Figure S10 in the Supporting Information.

FTIR measurements confirmed the structures. For example, HSS-12 (shown as Supporting Information Figure S11), along with the starting materials, were characterized. We also calculated the infrared bands of these materials to help make assignments, as indicated in Supporting Information Figure S12, within the same level of theory as that used for determining the electronic properties of these materials. It is in the 900–1200 cm^{-1} spectral window that differences are notable between the oligomer, comonomer and C_{60}. For HSS-12, a band centered at 1064 cm^{-1} is not present in the comonomer or C_{60}. The theoretical attribution of this band is at 1018 cm^{-1} and is due to the symmetric twisting of the C_{60}-comonomer groups *via* the linking methylenes and can be considered as a fingerprint of the polymerization link formed onto the sphere. More details exploring these data will be published in a forthcoming paper by our group.

CONCLUSIONS

The choice of this synthetic route is based on the ease of controlling the double-attack on fullerenes with the loss of only one double bond, and the current the lack of data on this relatively new synthetic path. It is demonstrated by molecular modeling that the expected electronic properties of ATRAP prepared PFs are similar to those of benchmark bis-modified C_{60} acceptors. The synthesis and characterization of the materials by CV would tend to confirm, at least in the first instance, this observation. This is suprising given the difference in structures and the loss of only one fullerene double bond with ATRAP as opposed to two for the standard bis-adducts. This work has also demonstrated that the ATRAP reaction is highly susceptible to the choice of comonomer used in terms of the molecular weights of the resulting oligomers and polymers. Of the series developed here, PFs with $-OC_{16}H_{33}$ comonomer side-chains display the highest molecular weights, and it can be expected that with optimizations even higher molecular weights may be obtained. In all cases, the oligomers and polymers are indicated by NMR to be relatively regioregular, although UV-visible spectroscopy indicates that of the series studied here, those with $-OC_{12}H_{25}$ side-chains are the most regioregular, and would be expected to have the best opto-electronic properties due to a reduced number of structural variations along each chain. These expected electronic properties and their ease of synthesis recommend them for use as electron acceptors and/or morphological stabilizers in BHJ OPV devices. This will be the focus of future work with this system.

ACKNOWLEDGMENTS

The research leading to these results has received funding from the European Union Seventh Framework Program (FP7/2011) under grant agreement no. 290022, from the Region Aquitaine (FULLINC 2011), from FAPESP (2011/02205-3) and from CAPES (BEX 11216-12-3). M. Pédeutour is warmly thanked for administrative support.

REFERENCES

1 B. van der Wiel, H.-J. Egelhaaf, H. Issa, M. Roos, N. Henze, *MRS Proceedings*, **2014**, 1639. DOI:10.1557/opl.2014.88.

2 A. Heeger, *J. Adv. Mater.* **2014**, *26*, 10.

3 B. Kippelen, J. L. Brédas, *Energy Environ. Sci.* **2009**, *2*, 251.

4 W. R. Wu, U. S. Jeng, C. J. Su, K. H. Wei, M. S. Su, M. Y. Chiu, C. Y. Chen, W. B. Su, C. H. Su, A. C. Su, *ACS Nano* **2011**, *5*, 6233.

5 D. Chen, A. Nakahara, D. Wei, D. Nordlund, T. P. Russell, *Nano Lett.* **2010**, *11*, 561.

6 Y. Xie, Y. Li, L. Xiao, Q. Qiao, R. Dhakal, Z. Zhang, Q. Gong, D. Galipeau, X. Yan, *J. Phys. Chem. C* **2010**, *114*, 14590.

7 W. Ma, C. Yang, X. Gong, K. Lee, A. Heeger, *J. Adv. Funct. Mater.* **2005**, *15*, 1617.

8 J. Nelson, *Mater. Today* **2011**, *14*, 462.

9 J. Peet, M. L. Senatore, A. J. Heeger, G. C. Bazan, *Adv. Mater.* **2009**, *21*, 1521.

10 D. Mark, J. Peet, T. Q. Nguyen, *J. Phys. Chem. C* **2008**, *112*, 7241.

11 J. S. Moon, C. J. Takacs, S. Cho, R. C. Coffin, H. Kim, G. C. Bazan, A. J. Heeger, *Nano Lett.* **2010**, *10*, 4005.

12 J. Peet, J. Y. Kim, N. E. Coates, W. L. Ma, D. Moses, A. J. Heeger, G. C. Bazan, *Nat. Chem.* **2007**, *6*, 497.

13 J. K. Lee, W. L. Ma, C. J. Brabec, J. Yuen, J. S. Moon, J. Y. Kim, K. Lee, G. C. Bazan, A. J. Heeger, *J. Am. Chem. Soc.* **2008**, *130*, 3619.

14 M. Urien, L. Bailly, L. Vignau, E. Cloutet, A. de Cuendias, G. Wantz, H. Cramail, L. Hirsh, J. P. Parneix, *Polym. Int.* **2008**, *57*, 764.

15 Sary, N. Richard, F. Brochon, C. Leclerc, N. Leveque, P. Audinot, J. N. Berson, S. Heiser, T. Hadziioannou, G. Mezzenga, *R. Adv. Mater.* **2010**, *22*, 763.

16 M. Muthukumar, C. K. Ober, E. L. Thomas, *Science* **1997**, *277*, 1225.

17 P. D. Topham, A. J. Parnell, R. C. Hiorns, *J. Polym. Sci., Part B: Polym. Phys.* **2011**, *49*, 1131.

18 M. Han, H. Kim, H. Seo, B. Ma, J. W. Park, *Adv. Mater.* **2012**, *24*, 6311.

19 M. Raïssi, H. Erothu, E. Ibarboure, H. Cramail, L. Vignau, E. Cloutet, R. C. Hiorns, *J. Mater. Chem. A* **2015**, *3*, 18207.

20 (a) H. H. Ramanitra, H. Santos Silva, B. A. Bregadiolli, A. Khoukh, C. M. S. Combe, S. A. Dowland, D. Bégué, C. F. O. Graeff, C. Dagron-Lartigau, A. Distler, G. E. Morse, R. C. Hiorns, *Macromolecules* **2016**, *49*, 1681; (b) M. Stephen, H. H. Ramanitra, H. Santos Silva, S. Dowland, D. Begue, K. Genevicius, K. Arlauskas, G. Juska, G. E. Morse, A. Distler, R. C. Hiorns, *Chem.*

Commun. **2016**, *52*, 6107; (c) M. Stephen, S. Dowland, A. Gregori, H. R. Ramanitra, H. Santos Silva, C. M. S. Combe, D. Bégué, C. Dagron-Lartigau, K. Genevičius, K. Arlauskas, G. Juška, A. Distler, R. C. Hiorns, *Polym. Int.* DOI: 10.1002/pi.5273.

21 N. Martín, F. Giacalone, Fullerene Polymers: Synthesis Properties and Applications; Wiley-VCH Verlag GmbH & Co, Weinheim, **2009**.

22 U. Reuther, T. Brandmueller, W. Donaubauer, F. Hampel, A. Hirsch, *Chem. Euro. J.* **2002**, *8*, 2261.

23 M. H. Liao, Y. Y. Lai, Y. Y. Lai, Y. T. Chen, C. E. Tsai, W. W. Liang, Y. J. Cheng, *ACS Appl. Mater. Interfaces* **2014**, *6*, 996.

24 C. Mathis, S. Nunige, F. Audouin, R. Nuffer, *Synth. Met.* **2001**, *121*, 1153.

25 F. Audouin, S. Nunige, R. Nuffer, C. Mathis, *Synth. Met.* **2001**, *121*, 1149.

26 F. Audouin, R. Nuffer, C. Mathis, *J. Polym. Sci. Pt A: Polym. Chem.* **2004**, *42*, 4820.

27 C. Mathis, B. Schmaltz, M. Brinkmann, *C. R. Chim.* **2006**, *9*, 1075.

28 P. Zhou, G. Q. Chen, H. Hong, F. S. Du, Z. C. Li, F. M. Li, *Macromolecules* **2000**, *33*, 1948.

29 R. C. Hiorns, E. Cloutet, E. Ibarboure, L. Vignau, N. Lemaitre, S. Guillerez, C. Absalon, H. Cramail, *Macromolecules* **2009**, *42*, 3549.

30 R. C. Hiorns, E. Cloutet, E. Ibarboure, A. Khoukh, H. Bejbouji, L. Vignau, H. Cramail, *Macromolecules* **2010**, *43*, 6033.

31 H. H. Ramanitra, B. A. Bregadiolli, H. Santos Silva, D. Bégué, C. F. O. Graeff, H. Peisert, T. Chassé, S. Rajoelson, M. Salvador, A. Osvet, C. J. Brabec, H. J. Egelhaaf, G. Morse, A. Distler, R. C. Hiorns, *J. Mater. Chem. C* **2016**, *4*, 8121.

32 O. F. Pozdnyakov, A. O. Pozdnyakov, B. Schmaltz, C. Mathis, *Polymer* **2006**, *47*, 1028.

33 J. C. Hummelen, B. W. Knight, F. LePeq, F. Wudl, J. Yao, C. J. Wilkins, *J. Org. Chem.* **1995**, *60*, 532.

34 C. M. Björström, A. Bernasik, J. Rysz, A. Budkowski, S. Nilsson, M. Svensson, M. R. Andersson, K. O. Magnusson, *J. Phys.: Condens. Matter* **2005**, *17*, L529.

35 E. Voroshazi, B. Verreet, A. Buri, R. Müller, D. Di Nuzzo, P. Heremans, *Org. Electron.* **2011**, *12*, 736.

36 L. Ye, S. Zhang, D. Qian, Q. Wang, J. Hou, *J. Phys. Chem. C* **2013**, *117*, 25360.

37 Y. Li, *Acc. Chem. Res.* **2012**, *45*, 723.

38 Y. He, Y. Li, *Phys. Chem. Chem. Phys.* **2011**, *13*, 1970.

39 Y. He, H. Y. Chen, J. Hou, Y. Li, *J. Am. Chem. Soc.* **2010**, *132*, 1377.

40 G. Zhao, Y. He, Y. Li, *Adv. Mater.* **2010**, *22*, 4355.

41 M. C. Scharber, D. Mühlbacher, M. Koppe, P. Denk, C. Waldauf, A. J. Heeger, C. J. Brabec, *Adv. Mater.* **2006**, *18*, 789.

42 D. K. Susarova, A. E. Goryachev, D. V. Novikov, N. N. Dremova, S. M. Peregudova, F. Razumov, P. A. Troshin, *Solar Energy Mater. Solar Cells* **2014**, *120*, 30.

43 M. Hee Yun, G. H. Kim, C. Yang, J. Y. Kim, *J. Mater. Chem.* **2010**, *20*, 7710.

44 (a) A. D. Becke, J. Chem. Phys. **1993**, *98*, 5648; (b) W. Lee-Yang, R. G. Parr, *Phys. Rev. B* **1988**, *37*, 785; (c) W. J. Hehre, R. Ditchfield, J. A. Pople, *J. Chem. Phys.* **1972**, *56*, 2257 (d) F. Neese, *Wiley Interdiscip. Rev.: Comput. Mol. Sci.* **2012**, *2*, 73.

45 N. Treitel, R. Shenhar, I. Aprahamian, T. Sheradsky, M. Rabinovitz, *Phys. Chem. Chem. Phys.* **2004**, *6*, 1113.

46 M. C. Scharber, D. Mühlbacher, M. Koppe, P. Denk, C. Waldauf, A. J. Heeger, C. Brabec, *J. Adv. Mater.* **2006**, *18*, 789.

47 C. J. Brabec, A. Cravino, D. Meissner, N. S. Sariciftci, T. Fromherz, M. T. Rispens, L. Sanchez, J. C. Hummelen, *Adv. Funct. Mater.* **2001**, *11*, 374.

48 A. Facchetti, M. H. Yoon, C. L. Stern, H. E. Katz, T. Marks, *J. Angew. Chem. Int. Ed.* **2003**, *42*, 3900.

49 M. J. Robb, S.-Y. Ku, F. G. Brunetti, C. J. Hawker, J. Polym. Sci. Pt A: Polym. Chem. **2013**, *51*, 1263.

50 K. Takimiya, I. Osaka, M. Nakano, *Chem. Mater.* **2013**, *26*, 587.

51 R. Stowasser, R. J. Hoffmann, *Am. Chem. Soc.* **1999**, *121*, 3414.

52 E. J. Baerends, O. V. Gritsenko, *J. Phys. Chem. A* **1997**, *101*, 5383.

53 A. M. Nardes, A. J. Ferguson, J. B. Whitaker, B. W. Larson, R. E. Larsen, K. Maturová, P. A. Graf, O. V. Boltalina, S. H. Strauss, N. Kopidakis, *Adv. Funct. Mater.* **2012**, *22*, 4115.

54 M. Lenes, G.-J. A. H. Wetzelae, F. B. Kooistra, S. C. Veenstra, J. C. Hummelen, P. W. M. Blom, *Adv. Mater.* **2008**, *20*, 2116.

55 M. Anafcheh, R. Ghafouri, N. L. Hadipour, *Solar Energy Mater. Solar Cells* **2012**, *105*, 125.

56 R. G. Parr, L. v. Szentpály, S. Liu, *J. Am. Chem. Soc.* **1999**, *121*, 1922.

57 R. A. Marcus, *J. Chem. Phys.* **1956**, *24*, 966.

58 Y. K. Lan, C. H. Yang, H. C. Yang, *Polym. Int.* **2010**, *59*, 16.

59 J. L. Brédas, D. Beljonne, V. Coropceanu, J. Cornil, *Chem. Rev.* **2004**, *104*, 4971.

60 R. Sure, S. Grimme, *J. Comput. Chem.* **2013**, *34*, 1672.

61 M. Chikamatsu, S. Nagamatsu, Y. Yoshida, K. Saito, K. Yase, K. Kikuchi, *Appl. Phys. Lett.* **2005**, *87*, 203504.

62 X. Meng, Q. Xu, W. Zhang, Z. Tan, Y. Li, Z. Zhang, L. Jiang, C. Shu, C. Wang, *ACS Appl. Mater. Interfaces* **2012**, *4*, 5966.

63 T. Nakanishi, Y. Shen, J. Wang, S. Yagai, M. Funahashi, T. Kato, P. Fernandes, H. Möhwald, *J. Am. Chem. Soc.* **2008**, *130*, 9236.

64 L. Schmidt-Mende, A. Fechtenkötter, K. Müllen, E. Moons, R. H. Friend, J. D. MacKenzie, *Science* **2001**, *293*, 1119.

65 S. Kumar, E. J. Wachtel, E. Keinan, *J. Org. Chem.* **1993**, *58*, 3821.

66 S. Sergeyev, W. Pisula, Y. H. Geerts, *Chem. Soc. Rev.* **2007**, *36*, 1902.

67 L. Y. Chen, F. H. Chien, Y. W. Liu, W. Zheng, C. Y. Chiang, C. Y. Hwang, C. W. Ong, Y. K. Lan, H. C. Yang, *Org. Elect.* **2013**, *14*, 2065.

68 C. Yang, J. K. Lee, A. J. Heeger, F. Wudl, *J. Mater. Chem.* **2009**, *19*, 5416.

69 R. S. Ruoff, D. S. Tse, R. Malhotra, D. C. Lorents, *J. Phys. Chem.* **1993**, *97*, 3379.

70 G.-W. Wang, K. Komatsu, Y. Murata, M. Shiro, *Nature* **1997**, *387*, 583.

71 A. M. Rao, P. Zhou, K. A. Wang, G. H. Hager, J. M. Holden, Y. Wang, W. T. Lee, X. X. Bi, P. C. Ecklund, D. S. Cornett, *Science* **1993**, *259*, 955.

72 H. Okamura, T. Terauchi, M. Minoda, T. Fukuda, K. Komatsu, *Macromolecules* **1997**, *30*, 5279.

73 S. Jiang, G. Singh, *Tetrahedron* **1998**, *54*, 4697.

74 H. Okamura, Y. Murata, M. Minoda, K. Komatsu, T. Miyamoto, T. S. M. Wan, *J. Org. Chem.* **1996**, *61*, 8500.

75 H. M. Wang, G. Wenz, J. Beilstein, *Org. Chem.* **2012**, *8*, 1644.

76 S. Fukuzumi, H. Mori, T. Suenobu, H. Imahori, X. Gao, K. M. Kadish, *J. Phys. Chem. A* **2000**, *104*, 10688.

77 S. Fukuzumi, T. Suenobu, X. Gao, K. M. Kadish, *J. Phys. Chem. A* **2000**, *104*, 2908.

78 K. M. Kadish, X. Gao, E. Van Caemelbecke, T. Suenobu, S. Fukuzumi, *J. Am. Chem. Soc.* **2000**, *122*, 563.

79 K. M. Kadish, X. Gao, E. Van Caemelbecke, T. Hirasaka, T. Suenobu, S. Fukuzumi, *J. Phys. Chem. A* **1998**, *102*, 3898.

80 F. Audouin, R. Nuffer, C. Mathis, *J. Polym. Sci. Pt A: Polym. Chem.* **2004**, *42*, 3456.

81 A. Gügel, P. Belik, M. Walter, A. Kraus, E. Harth, M. Wagner, J. Spickermann, K. Müllen, *Tetrahedron* **1996**, *52*, 5007.

82 K. M. Kadish, X. Gao, E. Van Caemelbecke, T. Suenobu, S. Fukuzumi, *J. Phys. Chem. A* **2000**, *104*, 3878.

83 P. K. Dhal, G. N. Babu, *Polym. Degrad. Stab.* **1987**, *18*, 1.